Double axial stabilization of a carbenium ion via convergent P=O→C⁺ tetrel bonding

Elishua D. Litle[a] and François P. Gabbaï*[a]

Received 00th January 20xx,
Accepted 00th January 20xx

DOI: 10.1039/x0xx00000x

Abstct: Our efforts in carbocation chemistry have led us to target examples of such species stabilized intramolecularly by tetrel bonding. Described here is an example of such a compound in which a triaryl carbenium is stabilized intramolecularly by two convergent P=O→$C_{carbenium}$ interactions, as confirmed by structural studies. The formation of this new motif favorably impacts the reversibility of the first and second reduction of the carbenium center. It also has profound influence on the Lewis acidity of the carbenium center which is lower than that of the unsubstituted parent carbenium by seven orders of magnitude.

The atypical bonding in pentacoordinate carbon species has attracted interest due to its relevance to the transition state (TS) of the common bimolecular nucleophilic substitution (S_N2) reaction (**Figure 1**).[1] These reactions proceed through a linear three-centre four-electron (3c-4e) TS, in which the carbon atom can be seen as adopting a "hypervalent" bonding configurations.[2] Drawn by this unusual bonding and aiming to provide models of this TS, several groups have targeted the synthesis of stable molecules featuring such a hypervalent, 10-electron, carbon centre.[3] These efforts have led to the isolation of **A** in which a dimethoxycarbenium ion, positioned at the 9-position of an anthracene backbone, is flanked by two adjacent methoxy functionalities (**Figure 1**).[4, 5] Owing to the rigidity of the backbone, the central carbon atom adopts a trigonal bipyramidal geometry with the axial oxygen atoms positioned at an average distance of 2.44 Å. A longer C-O distance of 2.69 Å was observed in the case of **B**, which features a less constrained backbone and aryl substituents at both the carbon atom and ether functionalities.[6] While the structures of these complexes have been firmly established, the impact of axial coordination on the properties of the central carbon atoms has not been assessed. As part of our investigations in carbocation chemistry,[7, 8] we now report a derivative featuring a carbenium ion intramolecularly stabilized by two weak dative bonds involving adjacent phosphine oxide functionalities. In addition to describing the structures and bonding of this compound, we also report on the impact of coordination on the acidity of the carbenium centre as well as its electrochemical properties.

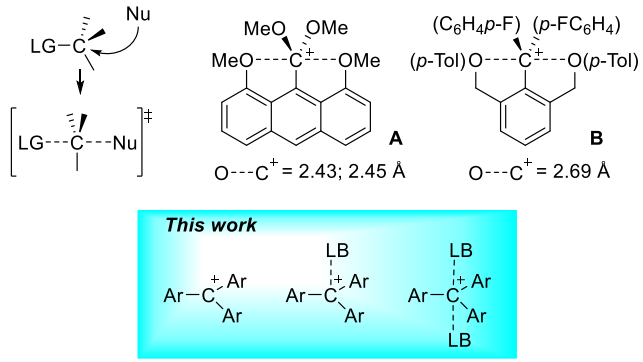

Figure 1. Top left: general scheme for the bimolecular nucleophilic substitution (S_N2) reaction. Top right: examples of isolated hypervalent carbeniums. Bottom: Schematic representation of the systems targeted in this study (LB = Lewis base).

To benchmark the properties of the aforementioned carbenium-bis(phosphine oxide) system to those of a simpler derivative, we first targeted a derivative in which the carbenium center is stabilized by a single P=O unit. Toward this end, the previously reported carbinol **1**,[9] dissolved in MeCN, was treated with H_2O_2 and subsequently HBF_4 to afford the monophosphine oxide analogue [**2**][BF_4] as an orange derivative. To access the bis(phosphine oxide) system, we first synthesized the bisphosphine carbinol **3** by allowing 2 equiv. of 1-lithio-2-diphenylphosphino-benzene to react with ethyl 4-(dimethylamino)benzoate (**Scheme 1**). Addition of H_2O_2 to a solution of **3** in MeCN, followed by treatment with HBF_4 led to a colour change from colourless to orange, indicating formation of the carbenium [**4**]$^+$ as a tetrafluoroborate salt. Transformation of the carbinols can be observed spectroscopically. Addition of hydrogen peroxide and HBF_4 leads to the disappearance of the OH proton resonance in the ^{1}H NMR spectrum. At the same time, ^{31}P NMR signal shifts from –16.0 ppm to 28.1 ppm upon conversion of **1** into [**2**][BF_4] and from –14.2 ppm to 28.4 ppm upon conversion of **3** into [**4**][BF_4]. The ^{13}C NMR signal of the central carbon, recorded at 25 °C, is also diagnostic, shifting from 84.05 ppm in **1** and 85.67 ppm in **3** to 176.35 ppm in [**2**][BF_4] and 175.48 ppm in [**4**][BF_4]. These downfield chemical shifts are close to that of [*p*-$Me_2NC_6H_4CPh_2$]$^+$ ([**5**]$^+$, 176.6 ppm), confirming the formation of a carbenium.[10] We also note that the position of these

[a] *Department of Chemistry, Texas A&M University, College Station, TX 77843, USA. E-mail: francois@tamu.edu*

† *Electronic supplementary information (ESI) available: Additional experimental and computational details and crystallographic data in cif format. CCDC 2296317-2296321. For ESI and crystallographic data in CIF or other electronic format see XXXXXXXXXXX*

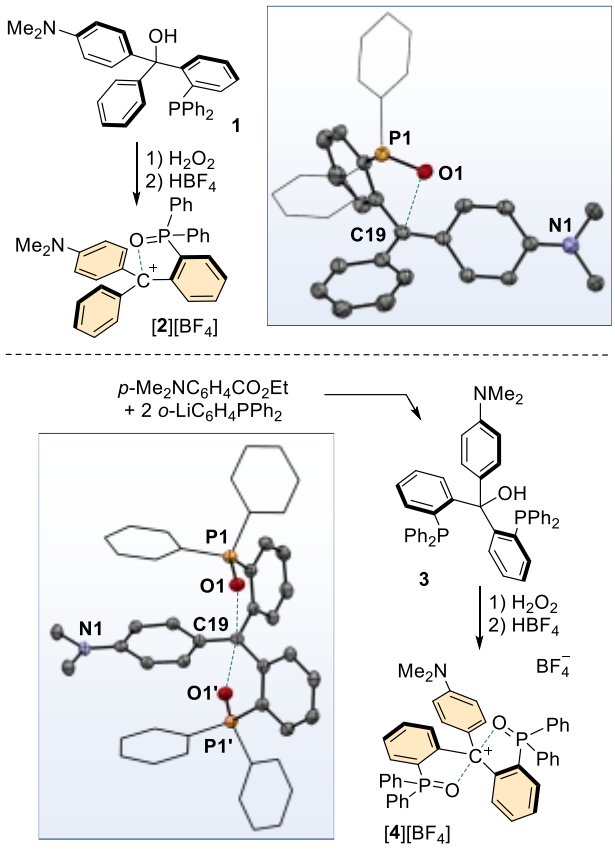

Scheme 1. Synthesis of [**2**][BF_4], **3**, and [**4**][BF_4] with an ORTEP drawing of the solid-state structure of [**2**][BF_4] and [**4**][BF_4]. BF_4^- counterion and hydrogen atoms omitted for clarity. Representative lengths for one of the independent molecules of [**2**][BF_4]: O1–C19: 2.872(6) Å. Representative bond angle and length for [**4**][BF_4]: O1–C19–O1': 171.6(2)°; O1–C19: 2.946(2) Å.

resonances show negligible changes upon elevation of the temperature (see SI).

The crystal structure of [**2**][BF_4] and [**4**][BF_4] have been determined using X-ray diffraction. In both structures, the central carbon exhibits a planar geometry. In the case of [**2**][BF_4], which possesses two independent molecules in the asymmetric unit, the phosphine oxide moiety occupies a position above the central carbon, indicating the presence of a P=O→$C_{carbenium}$ interaction. In a similar fashion, the structure of [**4**][BF_4] adopts a trigonal bipyramidal geometry where the phosphine oxide moieties occupy the axial positions above and below the plane containing the carbenium centre thus suggesting the presence of two convergent P=O→$C_{carbenium}$ interactions. The resulting C–O distances (2.872(6) Å and 2.902(6) Å for [**2**][BF_4]; 2.946(2) Å in [**4**][BF_4]) are within the sum of the van der Waals radii (3.25 Å)[11] but yet longer than in compounds **A** and **B** shown in **Figure 1**.[4, 6] The longer distances in [**2**][BF_4] and [**4**][BF_4] can be attributed to the decreased Lewis acidity of the carbenium due to the resonance stabilization provided by the dimethylamine group. However, they are comparable to the N→$C_{carbenium}$ bonds computed for intermolecular hypervalent carbenium systems featuring pyridine-like moieties as Lewis bases.[12] For example, the computed structure of the bis(pyridine) adduct of tritylium (**Figure 2**) exhibits N-C distances of 3.012 Å and 3.048 Å; slightly longer than the C-O distances calculated for [**2**][BF_4] and [**4**][BF_4] of 2.891 Å and 2.984 Å, respectively.

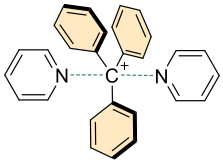

Figure 2. The bis(pyridine) tritylium complex calculated by Erdélyi *et al.* as a transition state.[12]

The nature of the P=O→$C_{carbenium}$ interactions present in [**2**]$^+$ and [**4**]$^+$ was probed using the atoms-in-molecules (AIM) method. In both systems, this method identifies bond paths connecting the oxygen atoms to the carbenium centers (**Figure 3**). These bond paths, characterized by an electron density (ρ(r)) at the bond critical point of 1.23×10^{-2} e/a_o^3 for [**2**]$^+$ and 1.05×10^{-2} e/a_o^3 for [**4**]$^+$ indicates the presence of a weaker interaction than in **A** (ρ(r) = 2.20×10^{-2} e/a_o^3) and **B** (ρ(r) = 1.70×10^{-2} e/a_o^3),[4, 6] in line with the elongated O→$C_{carbenium}$ distance in [**2**]$^+$ and

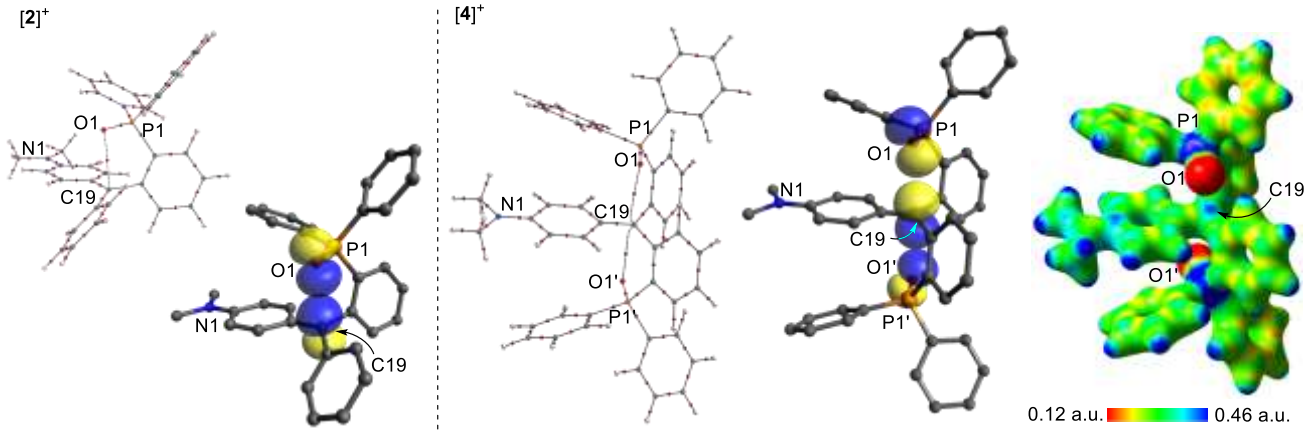

Figure 3. Left: AIM bond path between O→C19 with the bond critical point (ρ(r) = 1.23×10^{-2} e/a_o^3) and NBO orbitals of O→C19 interaction (E_2 = 6.64 kcal/mol) for [**2**]$^+$. Right: AIM bond paths between O→C19 interaction with the bond critical points (ρ(r) = 1.05×10^{-2} e/a_o^3); NBO orbitals of O→C19 interaction (E_2 = 4.01 kcal/mol), ESP map of [**4**]$^+$. ESP map was computed with an isovalue of 0.06, between 0.12 to 0.46 a.u.

$[\mathbf{4}]^+$. The slightly lower value found in $[\mathbf{4}]^+$ may be assigned to the formation of two O→$C_{carbenium}$ interactions that compete with one another.[13] The same effect can be held responsible for the magnitude of the O→$C_{carbenium}$ donor-acceptor interactions which are weaker in $[\mathbf{4}]^+$ (4.01 kcal/mol) than in $[\mathbf{2}]^+$ (6.64 kcal/mol), as derived from an NBO analysis. Inspection of the electrostatic surface potential (ESP) of $[\mathbf{4}]^+$ reveals the presence of p-hole on the central carbon, aligned with the negative surface regions adorned by the oxygen atom. This feature provides an illustration of the Coulombic contribution to the P=O→$C_{carbenium}$ interactions. We will note that the ESP map of $[\mathbf{4}]^+$ is very similar to that drawn for the aforementioned bis(pyridine) tritylium complex,[12] in which the N→$C_{carbenium}$ interactions were described as tetrel bonds,[14] a semantic choice made presumably to reflect on their weakness. By analogy, we propose that the P=O→$C_{carbenium}$ interactions in $[\mathbf{4}]^+$ can also be referred to as tetrel bonds. The ESP map of $[\mathbf{2}]^+$ displays similar characteristics, with the negative character of the oxygen atom surface facing its positive counterpart about the carbenium center, consistent with P=O→$C_{carbenium}$ (see SI).

The influence of this interaction can also be observed in the UV-vis spectra of $[\mathbf{2}][BF_4]$ and $[\mathbf{4}][BF_4]$.[10] Indeed, the λ_{max} varies with the stabilisation of the carbenium: there is a blue shift from the parent carbenium $[\mathbf{5}][BF_4]$ at 460 nm to 446 nm for $[\mathbf{2}][BF_4]$ and 432 nm for $[\mathbf{4}][BF_4]$. Given the stability of the isolated carbocations, we can experimentally study the influence of the P=O→$C_{carbenium}$ tetrel bonds on the electronic and chemical stability of $[\mathbf{2}][BF_4]$, and $[\mathbf{4}][BF_4]$. To elucidate the electronic impact of the P=O→$C_{carbenium}$ tetrel bonds, we studied $[\mathbf{2}][BF_4]$, $[\mathbf{4}][BF_4]$, and $[\mathbf{5}][BF_4]$ using cyclic voltammetry (CV) (**Figure 4**). Compound $[\mathbf{5}][BF_4]$ shows a reversible reduction at –0.87 V vs ferrocene/ferrocenium (Fc/Fc^+) in dichloromethane. The reduction shifts to more negative potentials with the addition of phosphine oxide moieties, with $[\mathbf{2}][BF_4]$ and $[\mathbf{4}][BF_4]$ exhibiting a reversible reduction at –0.93 V and –0.99 V, respectively.

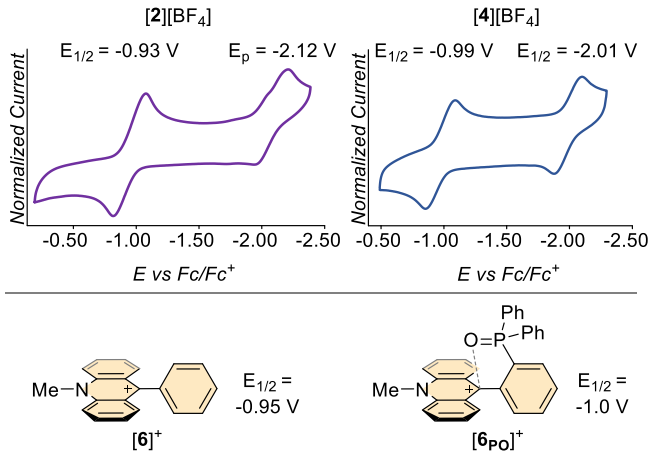

Figure 4. Top: CV of $[\mathbf{2}][BF_4]$ and $[\mathbf{4}][BF_4]$ in dichloromethane (Solutions of the concentration 5 x 10^{-4} M in dichloromethane with 100 mM $TBAPF_6$ as the supporting electrolyte). The feature in the CV of $[\mathbf{2}][BF_4]$ at ~-2 V has not been assigned. Bottom: Comparative data showing the structure and reduction potential (vs. Fc/Fc^+) of $[\mathbf{6}]^+$ and $[\mathbf{6}_{PO}]^+$.

We propose that the P=O→$C_{carbenium}$ tetrel bonds in $[\mathbf{2}][BF_4]$ and $[\mathbf{4}][BF_4]$ contribute to the moderate cathodic shift of the reduction potential. Such effects are not unprecedented and have been reported in the case the phosphine oxide-stabilized acridinium system $[\mathbf{6}_{PO}]^+$ which is shifted by 50 mV with respect to its unstabilized analog $[\mathbf{6}]^+$ (**Figure 4**).[8] In the case of $[\mathbf{4}][BF_4]$, this effect is augmented by the presence of two convergent P=O→$C_{carbenium}$ interactions. Both compounds feature a second reduction wave at –2.01 V for $[\mathbf{2}][BF_4]$ and –2.12 V for $[\mathbf{4}][BF_4]$ which appears to be pseudoreversible for the latter (**Figure 4**). We assign the increased reversibility of this wave to the steric protection provided by the two phosphine oxide moieties. Such steric protection effects have been invoked to explain the electrochemical formation of the perchlorotriphenylmethyl carbanion.[15]

Our investigations of $[\mathbf{2}][BF_4]$ and $[\mathbf{4}][BF_4]$ have allowed us to isolate their corresponding carbinols [**2**]OH and [**4**]OH which could be generated by addition of water. These two carbinols have been structurally characterized, providing unambiguous proof of their formation (see SI). Given the clean conversion of the carbenium cations $[\mathbf{2}]^+$ and $[\mathbf{4}]^+$ into their corresponding carbinols, we endeavored to measure their pK_{R^+} (**Figure 5**). Toward this end, $[\mathbf{2}][BF_4]$ and $[\mathbf{4}][BF_4]$ where titrated with NaOH in a H_2O/MeCN 9:1 (v/v) solvent mixture. These titrations, monitored by UV spectroscopy, afforded pK_{R^+} values of 5.03 for $[\mathbf{2}][BF_4]$ and 11.72 for $[\mathbf{4}][BF_4]$. To benchmark these results, we also evaluated the parent derivative $[\mathbf{5}][BF_4]$ under the same conditions and obtained a value of 4.40, close to that previously

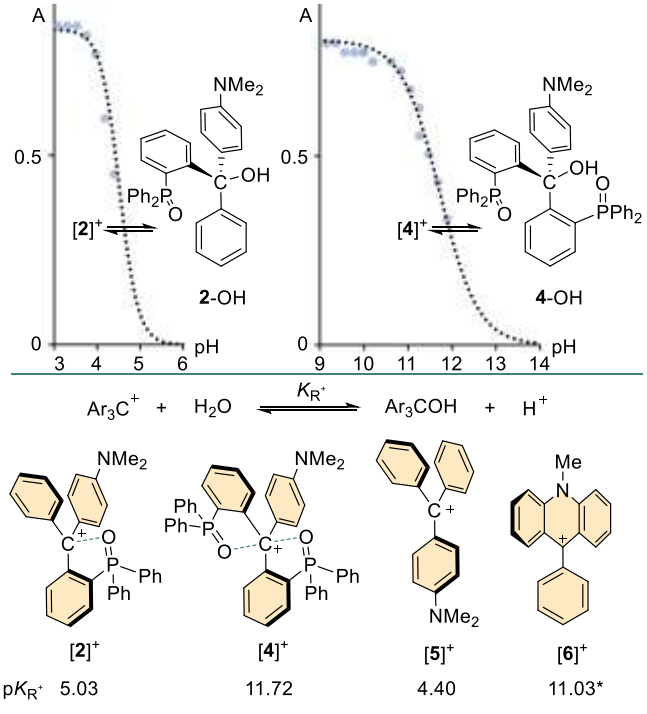

Figure 5. Top: Spectrophotometric titration data collected for $[\mathbf{2}][BF_4]$ and $[\mathbf{4}][BF_4]$ in H_2O/MeCN 9:1 (v/v). Bottom: Summary of pK_{R^+} data and comparison with that of $[\mathbf{6}]^+$. The * symbol indicates values taken from the literature.[16]

reported in the literature.[17] These results indicate that the P=O→$C_{carbenium}$ tetrel bond of [**2**][BF_4] weakly stabilizes the carbenium center against nucleophilic addition. By contrast, the addition of a second P=O→$C_{carbenium}$ interaction in the molecular design leads to a surprisingly large increase of the pK_{R^+} value which augments by seven orders of magnitude. Thus, the stabilization provided by this second tetrel bond affords a carbenium ion as stable as the 9-phenyl-*N*-methyacridinium cation ([**6**]$^+$),[16] a cation that derives its stability from the aromaticity of the carbenium unit. In other words, the convergent P=O→$C_{carbenium}$ tetrel bonds in [**4**][BF_4] passivates the carbenium center by hindering nucleophilic addition.

In summary, we have described a triarylcarbenium cation stabilized intramolecularly by two convergent P=O→$C_{carbenium}$ tetrel bonds. Despite their weakness, these bonds profoundly influence the Lewis acidity of the carbenium center as indicated by the pK_{R^+} of [**4**][BF_4] which is seven orders of magnitude higher than that of the parent derivative. Remarkably, the electrochemical properties of the carbenium ion are much less affected, suggesting double tetrel bonding as a strategy for the chemical stabilization of carbenium-based liquid electrolyte solutions in redox-flow batteries.[18]

Acknowledgements

We gratefully acknowledge support from the National Science Foundation (CHE-2154972) and the Welch Foundation (A-1423). All calculations were conducted with the advanced computing resources provided by Texas A&M High Performance Research Computing.

Conflicts of interest

There are no conflicts to declare.

References

1. P. Walden, *Ber. Dtsch. Chem. Ges.*, 1896, **29**, 133-138; W. A. Cowdrey, E. D. Hughes, C. K. Ingold, S. Masterman and A. D. Scott, *J. Chem. Soc.*, 1937, 1252-1271; L. Sun, W. L. Hase and K. Song, *J. Am. Chem. Soc.*, 2001, **123**, 5753-5756.
2. K.-Y. Akiba, *Chemistry of Hypervalent Compounds*, Wiley-VCH, New York, 1999; L. Tenud, S. Farooq, J. Seibl and A. Eschenmoser, *Helv. Chim. Acta*, 1970, **53**, 2059-2069; I. Lee, C. K. Kim, D. S. Chung and B.-S. Lee, *J. Org. Chem.*, 1994, **59**, 4490-4494.
3. T. R. Forbus, Jr. and J. C. Martin, *J. Am. Chem. Soc.*, 1979, **101**, 5057-5059; M. Hojo, T. Ichi and K. Shibato, *J. Org. Chem.*, 1985, **50**, 1478-1482.
4. K.-y. Akiba, M. Yamashita, Y. Yamamoto and S. Nagase, *J. Am. Chem. Soc.*, 1999, **121**, 10644-10645.
5. M. Yamashita, Y. Yamamoto, K.-y. Akiba, D. Hashizume, F. Iwasaki, N. Takagi and S. Nagase, *J. Am. Chem. Soc.*, 2005, **127**, 4354-4371.
6. K.-y. Akiba, Y. Moriyama, M. Mizozoe, H. Inohara, T. Nishii, Y. Yamamoto, M. Minoura, D. Hashizume, F. Iwasaki, N. Takagi, K. Ishimura and S. Nagase, *J. Am. Chem. Soc.*, 2005, **127**, 5893-5901.
7. H. Wang, C. E. Webster, L. M. Perez, M. B. Hall and F. P. Gabbaï, *J. Am. Chem. Soc.*, 2004, **126**, 8189-8196; H. Wang and F. P. Gabbaï, *Angew. Chem. Int. Ed.*, 2004, **43**, 184-187; C.-W. Chiu and F. P. Gabbaï, *Angew. Chem. Int. Ed.*, 2007, **46**, 1723-1725; L. C. Wilkins, Y. Kim, E. D. Litle and F. P. Gabbaï, *Angew. Chem. Int. Ed.*, 2019, **58**, 18266-18270; M. Karimi, R. Borthakur, C. L. Dorsey, C.-H. Chen, S. Lajeune and F. P. Gabbaï, *J. Am. Chem. Soc.*, 2020, **142**, 13651-13656; E. D. Litle and F. P. Gabbaï, *Angew. Chem. Int. Ed.*, 2022, **61**, e202201841; G. Park, M. Karimi, W.-C. Liu and F. P. Gabbaï, *Angew. Chem. Int. Ed.*, 2022, **61**, e202206265; E. D. Litle and F. P. Gabbaï, *Chem. Commun.*, 2023, **59**, 603-606.
8. W.-C. Liu, Y. Kim and F. P. Gabbaï, *Chem. Eur. J.*, 2021, **27**, 6701-6705.
9. E. D. Litle, L. C. Wilkins and F. P. Gabbaï, *Chem. Sci.*, 2021, **12**, 3929-3936.
10. M. Horn and H. Mayr, *Chem. Eur. J.*, 2010, **16**, 7469-7477.
11. A. Bondi, *J. Phys. Chem.*, 1964, **68**, 441-451.
12. A. Karim, N. Schulz, H. Andersson, B. Nekoueishahraki, A.-C. C. Carlsson, D. Sarabi, A. Valkonen, K. Rissanen, J. Gräfenstein, S. Keller and M. Erdélyi, *J. Am. Chem. Soc.*, 2018, **140**, 17571-17579.
13. T. Yamaguchi, Y. Yamamoto, D. Kinoshita, K.-y. Akiba, Y. Zhang, C. A. Reed, D. Hashizume and F. Iwasaki, *J. Am. Chem. Soc.*, 2008, **130**, 6894-6895.
14. S. Scheiner, *Phys. Chem. Chem. Phys.*, 2021, **23**, 5702-5717.
15. O. Armet, J. Veciana, C. Rovira, J. Riera, J. Castaner, E. Molins, J. Rius, C. Miravitlles, S. Olivella and J. Brichfeus, *J. Phys. Chem.*, 1987, **91**, 5608-5616; I. Ratera and J. Veciana, *Chem. Soc. Rev.*, 2012, **41**, 303-349.
16. J. W. Bunting, V. S. F. Chew, S. B. Abhyankar and Y. Goda, *Can. J. Chem.*, 1984, **62**, 351-354.
17. R. Breslow and W. Chu, *J. Am. Chem. Soc.*, 1973, **95**, 411-418.
18. J. Moutet, J. M. Veleta and T. L. Gianetti, *ACS Appl. Energy Mater.*, 2021, **4**, 9-14; J. Moutet, D. Mills, M. M. Hossain and T. L. Gianetti, *Materials Advances*, 2022, **3**, 216-223.

